

the signal background limited. To extract the luminescence signal, shown as the computed curve of Fig. 2, therefore, it was necessary to use the technique of comparing the sample curve with that of the barium sulfate reflectance standard.

The barium sulfate has a reflectance of very nearly 100 percent over the entire wavelength band investigated and is not known to have any significant luminescence in this band. Its curve, therefore, represents the spectrum of the light exciting the sample, and the ratio of the sample curve to that of barium sulfate is the sample reflectance. Any increase of apparent reflectance of the sample can be the result of either reflectance changes or luminescence or both. Comparison of such curves from all samples showed increases, and therefore possible luminescence, in the neighborhood of 5300, 5500, 3500 to 4100, 4300 and 4970 Å, in order of decreasing intensity. The 3500- to 4100-Å band, especially, is a region in which we have found granite and gabbro reflectance values to remain constant or to decrease, so that in this region, at least, the case for luminescence is strengthened. However, the effects are small and could arise from other than luminescence. In this event, the calculated efficiencies represent an upper limit for the samples for the conditions of this particular set of measurements.

The efficiencies are as follows: all lunar samples, $\leq 6 \times 10^{-5}$; granite, $\sim 10^{-4}$; gabbro, $\leq 8 \times 10^{-5}$; and willemite, $\sim 2 \times 10^{-2}$. The values represent total efficiencies; that is, the ratio of energy in the luminescent band to energy in the band incident upon the sample. Despite the uncertainty, the values shown are consistent in that the lunar samples, which are very similar to gabbro in composition, are also similar in apparent luminescence efficiency.

The outstanding feature of these results is the low values of the efficiencies for the lunar samples and the two terrestrial rocks. They are comparable to the terrestrial rock efficiencies that we and Nash measured with protons and that we measured with electrons and x-rays; they are also much lower than those we estimated for terrestrial rocks with the 1800- to 2200-Å band by a less refined filter method (6, 7). In our earlier study, with a 1 percent efficiency for the 1800 to 2200 Å band, we calculated a level of luminescence, 5 percent of the reflected background in the 2200 to 2500 Å band, that was the average observed around 3950 Å by Grainger (4),

who made the most accurate line-depth measurements of the moon. The efficiencies we measured in this study of the Apollo 11 lunar samples are more than two orders of magnitude lower; in a similar calculation they would yield a level of luminescence that would be undetectable by the line-depth technique. If our further studies with excitation at other ultraviolet wavelengths and with proton, electron, and x-ray excitation show no greater efficiencies than these, the Apollo 11 landing area can be considered to contribute little or nothing to the luminescence determined by the line-depth technique. Grainger's observations did not include the Apollo 11 landing area; if correct, they imply higher luminescence efficiencies on other areas of the moon. Terrestrial gabbros, which are similar in composition to the Apollo 11 rocks, are found in both this and previous studies to possess low luminescence efficiency as compared to granites. Therefore, other lunar areas, especially in the highlands, could contain rocks of higher efficiency than those from Apollo 11. In this connection, note that the Surveyor 7 alpha-scattering analysis measured less than half as much iron, a luminescence-quenching element, at the Tycho site than was measured at the Surveyor 5 and

6 mare sites (8). Finally, it is possible that certain excitation mechanisms that exist in the space environment, such as simultaneous irradiation with ultraviolet and charged particles, may result in higher efficiencies and await laboratory testing. For these reasons, samples from many areas of the moon need to be studied in order to characterize the luminescence of the lunar rocks and to understand its significance.

NORMAN N. GREENMAN

H. GERALD GROSS

*Space Sciences Department,
McDonnell Douglas Astronautics
Company—Western Division,
Santa Monica, California 90406*

References and Notes

1. F. Link, *Compt. Rend.* 223, 976 (1946).
2. N. A. Kozhev, *Izv. Crimean Astrophys. Obs.* 16, 148 (1956).
3. J. Dubois, *Rozpravy Cesk. Akad. Ved* 69, 1 (1959).
4. J. F. Grainger, *Astron. Contrib. Univ. Manchester.* 104, 1 (1963).
5. H. Spinrad, *Icarus* 3, 500 (1964).
6. N. N. Greenman, V. W. Burkig, H. G. Gross, J. F. Young, Douglas Aircraft Co. Rept. SM-48529 (1965).
7. D. B. Nash, *J. Geophys. Res.* 71, 2517 (1966).
8. A. L. Turkevich, W. A. Anderson, T. E. Economou, E. J. Franzgrote, H. E. Griffin, S. L. Grotch, J. H. Patterson, K. P. Sowinski, NASA SP-184 (1969).
9. Supported by NASA contract NAS9-7966. We wish to thank M. W. Wegner, W. M. Hansen, and A. D. Pinkul for their assistance in these studies.

4 January 1970

Luminescence and Reflectance of Tranquillity Samples: Effects of Irradiation and Vitrification

Abstract. Luminescence measurements of Tranquillity samples indicate that energy efficiencies for excitation by protons and ultraviolet are in the range 10^{-6} or below; natural and induced thermoluminescence is even weaker. If these samples are typical, lunar surface luminescence cannot occur at reported levels. Comparison of proton luminescence spectra from the exterior and interior of rocks and fine fragments provides evidence of solar wind impingement on the moon's surface. Spectral reflectance and albedo measurements of fresh rock powders before and after both laboratory proton irradiation and fusion indicate that vitrification may be an important mechanism of lunar darkening.

Experiments simulating solar wind proton irradiation and solar ultraviolet irradiation on the moon's surface were performed to determine the emission properties and energy efficiencies of luminescence and thermoluminescence as well as the effects of irradiation and vitrification on spectral reflectance (0.23 to 2.5 μm) and albedo. Samples examined (1) represent each of the three rock types and fine soil collected (2).

Samples were handled and prepared in dry N_2 . This was later omitted when experiments showed no detectable

effects on any of our measurements from exposure to air. Proton and ultraviolet irradiations were conducted in vacuum at 10^{-6} torr. Thermoluminescence and spectral reflectance measurements were made with instruments flushed with dry N_2 .

Irradiations were carried out with 1-, 2-, and 4-keV protons (to simulate solar wind) at fluxes in the range 3 to 10×10^{13} protons $\text{cm}^{-2} \text{sec}^{-1}$ (~ 5 to $15 \mu\text{a cm}^{-2}$) for doses of up to 4×10^{19} protons cm^{-2} (equivalent to 2×10^4 years of solar wind) per sample, and simultaneously and independently with

0.25 to 0.43 μm ultraviolet at solar equivalent intensity ($\sim 10^5$ ergs cm^{-2} sec^{-1}). Luminescence spectra and energy efficiency (3) in the range 0.25 to 0.72 μm were measured with a calibrated grating monochromator and a photomultiplier with S 20 response. Rapid spectral scanning capability allowed complete luminescence spectra to be recorded every 10 sec in order to measure the rapid changes in relative spectral intensity exhibited by silicate luminescence during initial proton excitation (4).

Proton-excited luminescence was observed in all rock and soil samples. Initial spectra from both fresh crystalline rock material and freshly crushed soil fragments show two emission bands of nearly equal intensity in the blue at 0.40 μm and yellow at 0.55 μm . With continued irradiation the spectra decrease in intensity and change in relative spectral distribution with disappearance of the yellow band and shift in the peak position of the blue band to 0.46 μm . This behavior is similar to that observed for terrestrial and meteoritic silicates (4) and for convenience will be referred to as luminescence decay. The resulting spectra will be referred to as decayed spectra.

Energy efficiencies at initial laboratory proton excitation are in the range 1 to 6×10^{-6} for bulk samples and 2.4×10^{-5} for a plagioclase mineral separate; these values are low in the range of values determined for terrestrial and meteoritic silicates (5). Efficiency for a given sample decreases with increasing proton dose, proton energy density, and sample temperature. Most of the luminescence from lunar samples is produced by the plagioclase mineral component. Since all samples examined contain plagioclase in varying amounts, all spectra are similar in shape. Typical spectra at initial excitation by 2.0-keV protons are shown in Fig. 1 along with corresponding values of integral energy efficiencies. From sample to sample, efficiency increases with increasing plagioclase and decreasing Fe and glass concentrations. Crushed artificial glass, made by fusing (6) a small portion of sample 10020, yields no detectable proton-excited luminescence.

The luminescence data obtained, if typical for the whole moon, confirm that it is impossible for solar wind or flare proton bombardment to excite luminescence from rocks and soil on the moon's sunlit surface that would be

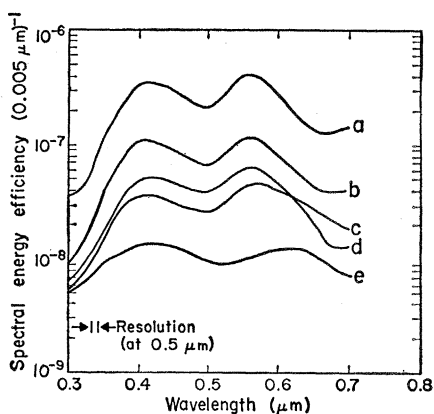


Fig. 1. Proton-excited luminescence spectra for Tranquillity samples at initial exposure to laboratory irradiation. 2.0-keV proton excitation, $15 \mu\text{a cm}^{-2}$ ($\sim 10^{14}$ protons cm^{-2} sec^{-1}). Samples powdered to $< 50 \mu\text{m}$. Pressure 2×10^{-6} torr. Temperature 50°C . Curve *a*, plagioclase from medium-grained igneous sample 10058, integral energy efficiency 2.4×10^{-5} . Curve *b*, medium-grained igneous sample 10058, integral energy efficiency 5.6×10^{-6} . Curve *c*, 0.15 to 1.0-mm crushed fines, integral energy efficiency 2.5×10^{-6} . Curve *d*, fine-grained igneous sample 10020, integral energy efficiency 3.0×10^{-6} . Curve *e*, 1.0-mm uncrushed fines, integral energy efficiency 0.9×10^{-6} .

detectable from the earth. Figure 2 illustrates the energy relationship between incident proton intensity, luminescence intensity, and required brightness levels to account for reports of lunar luminescence (7) by various observational techniques. Note that even at laboratory proton intensities, which are $\sim 10^5$ times greater than maximum solar intensity, the required brightness is too low by approximately two orders of magnitude. At lower proton intensity the luminescence energy efficiency increases (Fig. 2), but the luminescence brightness decreases; at equivalent solar wind or solar flare intensity the extrapolated luminescence efficiency of lunar material is in the range 0.1 to 1.0 percent, but the luminescence brightness would be too low for observation by five orders of magnitude. Luminescence efficiency of 100 percent would be insufficient to account for reported observations, as pointed out in previous studies (8).

The exterior surfaces of lunar crystalline rocks, the microbreccia, and the uncrushed fines tend to yield decayed luminescence spectra and low efficiencies at initial laboratory proton irradiation relative to the spectra from fresh interiors of crystalline rocks and freshly crushed fines. This is especially evidenced by absence or relative weak-

ness of the yellow (0.55 μm) band in the initial spectra. The top exterior surfaces of 10058, 10020, and 10057 and the bottom of 10058 show decayed spectra, while the bottom of 10020 gives a fresh spectrum.

The decayed proton luminescence spectra suggest that these particular crystalline rock surfaces, breccia materials, and fines have been exposed to low-keV ion irradiation on the moon's surface, presumably from the solar wind. Comparison of natural and laboratory decayed spectra indicates that the incident solar wind doses required to produce the natural decayed spectra are $> 10^{16}$ protons cm^{-2} . The luminescence spectra observed in the laboratory therefore provide direct evidence for impingement of solar wind ions on the moon's surface and may be a qualitative measure of the minimum time of exposure of lunar material surfaces to the solar wind. The quantitative aspects of this concept, however, require further study. The fact that fines uniformly give decayed spectra suggests sufficient tilling of the lunar regolith at least to the depth sampled to permit solar wind exposure of all fine particles, top and bottom, to $> 10^{16}$ ions cm^{-2} ; but all rocks (e.g., 10020) were not uniformly exposed in the process.

Ultraviolet-excited luminescence was undetectable in all samples examined, putting an upper limit on the energy efficiency at about 10^{-6} . Likewise, simultaneous ultraviolet and proton irradiation was no more effective in exciting luminescence than the proton irradiation alone. If these results are typical for the moon, solar ultraviolet irradiation alone or together with the solar wind cannot yield detectable lunar luminescence in rocks and soil.

Natural thermoluminescence (9) below 120°C was absent in all samples examined; some natural thermoluminescence above 120°C was observed in sample 10058. Low-level induced thermoluminescence was achieved by x-ray exposure of crystalline material (10020 and 10058); storage efficiencies (3) are in the range 10^{-12} to 10^{-11} for the temperature range 23° to 500°C . No thermoluminescence could be induced with x-rays in soil or breccia. Ultraviolet exposure equivalent to 4 days of solar-ultraviolet exposure induced no detectable thermoluminescence in sample 10058. Proton irradiation (1×10^{18} protons cm^{-2} at 2 keV and 5×10^{16} protons cm^{-2} at 4 keV) yielded no induced thermoluminescence. The pos-

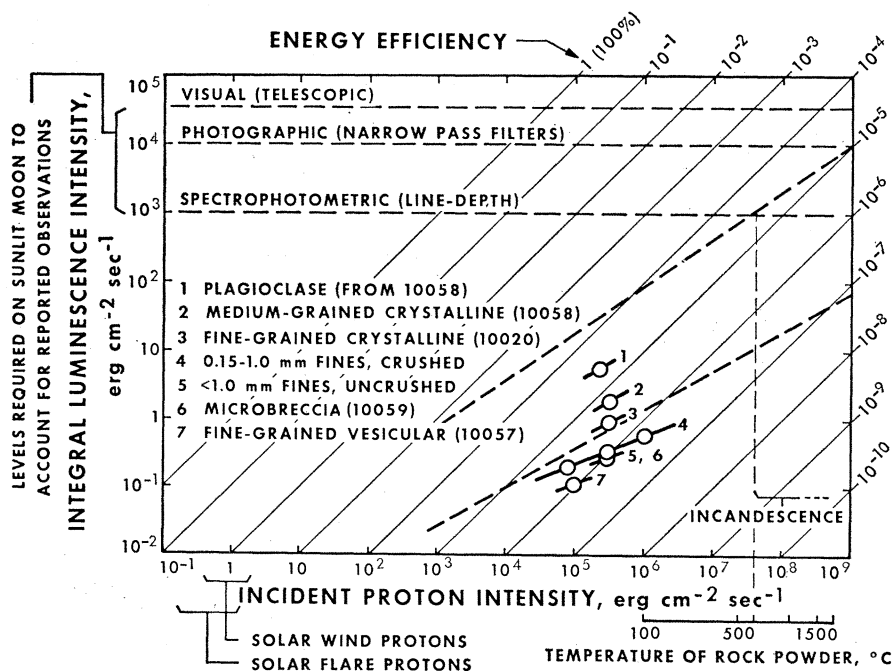


Fig. 2. Summary of the solar-proton excited lunar luminescence detection problem. Light solid diagonal lines indicate energy efficiency. Dashed diagonal lines show upper and lower bounds of luminescence efficiency trends for terrestrial and meteorite silicate rocks under various proton intensities (5). Intense proton flux causes rock material to incandesce before luminescing bright enough for detection on the sunlit moon from earth (5). Solar flare protons, although higher in energy per ion, amount to lower total energy flux than solar wind protons.

sible occurrence of detectable thermoluminescence on the moon near the lunar dawn terminator has been suggested (10). The present data indicate that the storage efficiency of lunar material is many orders of magnitude too low to yield levels of emission that would be detectable on the lunar surface against a background of either direct solar illumination or earthshine.

Spectral reflectance and albedo (11) were measured to determine how proton irradiation experiments affect the reflecting properties of lunar material and if such irradiation could alter the reflectance of fresh crushed rocks and glass to that of average lunar soil. Much of the soil was found to consist of glass, which presumably formed in part from crystalline parent material

(judging from glass-lined pits and glass spatters on crystalline rocks). To determine the effects of irradiation on the reflectance and albedo of fresh glass, a representative sample of lunar crystalline material (10020) was fused (6). Glass and parent material were both ground to $< 50 \mu\text{m}$ and subjected to a 2-key proton irradiation of 4×10^{19} protons cm^{-2} for crystalline material and 2×10^{19} protons cm^{-2} for the glass. Reflectance spectra before and after irradiation are shown in Figs. 3 and 4. The reflectance of crystalline material has a prominent minimum near $1.0 \mu\text{m}$, other subtle structures near 1.25 and $2.2 \mu\text{m}$, and a suggestion of structure around $1.7 \mu\text{m}$. In glass there are broad minimums at ~ 1.02 and $1.8 \mu\text{m}$. By comparison, fine soil material shows subtle structure near $0.95 \mu\text{m}$. In the visible, glass shows a pronounced enhancement in the red compared with unfused material. Elsewhere the spectra are relatively featureless. In all spectral regions the reflectance of glass is less than that of the original crystalline sample.

The experimental proton irradiations have reduced the spectral reflectance of both crystalline and artificial glass materials in the infrared below about $1.5 \mu\text{m}$ and uniformly in the visible; indicated changes in the ultraviolet reflectance of glass are within experimental uncertainty. The irradiation reduced the albedo of the crystalline material from 20 to 17 percent, and that of the glass from 8 to 5 percent; vitrification alone changes the albedo from 20 to 8 percent for the sample studied.

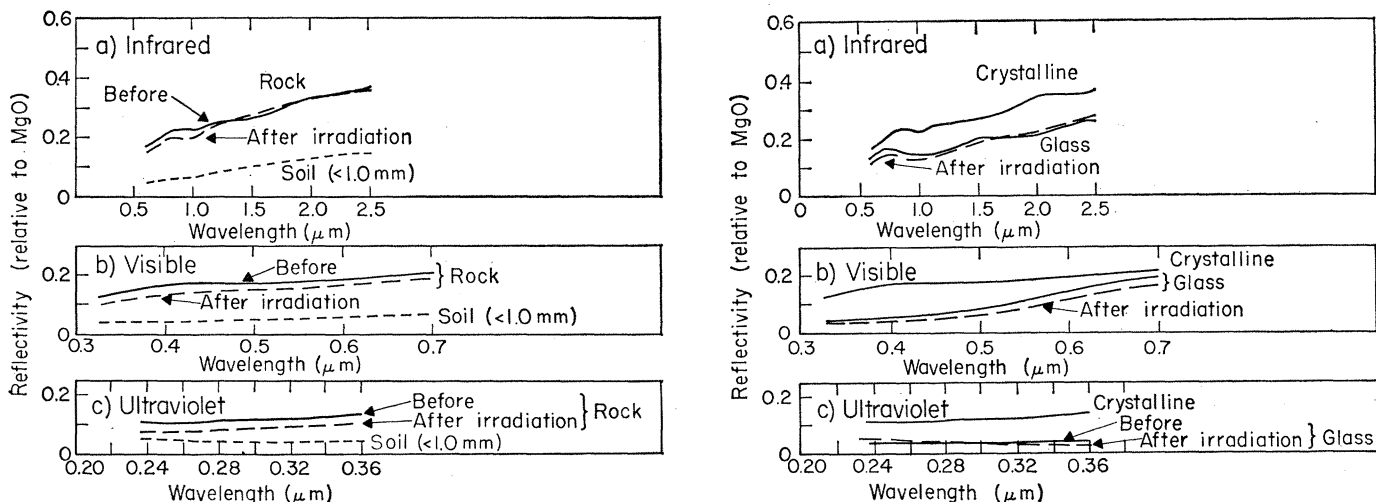


Fig. 3 (left). Reflectance spectra of crushed fine-grained crystalline material (10020), powdered to $< 50 \mu\text{m}$, before and after bombardment simulating about 2×10^4 years of solar wind. Irradiation 2-key protons, $4 \times 10^{19} \text{cm}^{-2}$. Spectra of natural lunar soil are shown for comparison. Fig. 4 (right). Reflectance spectra of fine-grained crystalline material (10020) powdered to $< 50 \mu\text{m}$, its glass equivalent, and glass after proton irradiation simulating about 1×10^4 years of solar wind exposure. Glass irradiation 2-key protons, $2 \times 10^{19} \text{cm}^{-2}$.

The cause of experimental proton irradiation darkening is not understood, but contamination is suspected to play a role (12). We are thus cautious in asserting that proton irradiation produces significant lunar darkening. Alternatively, vitrification may be an important darkening process. Except in the ultraviolet, neither the experimental irradiation dose nor the artificial vitrification alone produces material with the reflectance properties of lunar soil.

DOUGLAS B. NASH
JAMES E. CONEL

RAYMOND T. GREER*
Jet Propulsion Laboratory,
Pasadena, California 91103

References and Notes

1. Lunar Receiving Laboratory rocks numbered 10058 (medium-grained igneous), 10020 (fine-grained igneous), 10057 (fine-grained vesicular), 10059 (microbreccia), and fines < 1.0 mm. All samples were received packaged in N₂, rock samples as 1- to 1.5-g chips from top exterior, bottom exterior, and interior of each rock.
2. Lunar Sample Preliminary Examination Team, *Science* 165, 1211 (1969).
3. Energy efficiency is defined as the ratio of integral luminescence energy to applied proton energy. Thermoluminescence storage efficiency is defined here as the ratio of total thermoluminescence energy observed to total applied x-ray, ultraviolet, or proton energy prior to trap saturation.

4. D. B. Nash, *J. Geophys. Res.* 71, 2517 (1966); J. E. Geake and G. Walker, *Geochim. Cosmochim. Acta* 30, 929 (1966).
 5. D. B. Nash, *ibid.*; D. B. Nash, in *Thermoluminescence of Geological Materials*, D. J. McDougall, Ed. (Academic Press, New York, 1968), p. 587.
 6. Glass was fused in dry nitrogen using a platinum vessel after slow heating to drive off adsorbed atmospheric constituents.
 7. Z. Kopal and T. W. Rackham, *Icarus* 2, 481 (1963); J. F. Grainger and J. Ring, *Proc. Intern. Space Sci. Symp.*, W. Priester, Ed. (North-Holland, Amsterdam, 1963), p. 989; H. Spinrad, *Icarus* 3, 500 (1964); T. B. McCord, *J. Geophys. Res.* 72, 2087 (1967).
 8. E. J. Flam and R. E. Lingenfelter, *Nature* 205, 1301 (1965); D. B. Nash, *ibid.* (1966); E. P. Ney, N. J. Woolf, R. J. Collins, *J. Geophys. Res.* 71, 1787 (1966).
 9. Thermoluminescence was measured using an RCA 6199 photomultiplier and a heating rate of 80°C min⁻¹.
 10. K. H. Sun and J. L. Gonzalez, *Nature* 212, 23 (1966); M. Sidran, *J. Geophys. Res.* 73, 5195 (1968).
 11. Hemispherical spectral reflectance was measured with a Beckman DK-2A spectroradiometer modified to accept horizontal, uncovered samples. Albedo, defined here as the bidirectional integral reflectance (0.4 to 0.7 μm) measured with vertical illumination and phase angle of 15°, was determined with a goniophotometer. All measurements were made relative to fresh smoked MgO.
 12. D. B. Nash, *J. Geophys. Res.* 72, 3089 (1967).
 13. We thank Clay Seaman, Warren Rachwitz, Fraser Fanale, Elsa Abbott, Edgar Bollin, and Charles Fisher for their assistance. This research under NASA contract NAS 7-100.
- * National Research Council Resident Research Associate appointed to the Jet Propulsion Laboratory. Present address: Department of Nuclear Engineering, Iowa State University, Ames 50010.
- 4 January 1970

Thermal Radiation Properties and Thermal Conductivity of Lunar Material

Abstract. The thermal radiation properties were measured for lunar fines and chips from three different lunar rocks. Measurements for the fines were made at atmospheric pressure and at a pressure of 10⁻⁵ torr or lower. The directional reflectance was obtained over a wavelength range of 0.5 to 2.0 microns for angles of incidence up to 60 degrees. The bidirectional reflectance—the distribution of reflected light—was measured for white light angles of illumination up to 60 degrees. The thermal conductivity was measured over a temperature range 200 to 400°K under vacuum conditions.

Directional reflectances of Apollo 11 lunar fines and rock chips are presented for white light and for wavelengths from 0.5 to 2.0 μm. The measure-

ments include the directional reflectance (1), $\rho(\psi)$, and the normalized bidirectional reflectance (2), $\rho_b(\psi, \theta)$. The directional reflectance subtracted from

unity gives the absorptance as a function of angle of illumination; the bidirectional reflectance indicates the distribution of reflected light as a function of angles of illumination and viewing. Both quantities are needed for calculations of thermal energy balance.

A second thermophysical property, the thermal conductivity of the fines, k , was measured under vacuum conditions for temperatures from 205° to 404°K. This property, like the reflectance, is needed for thermal energy balance calculations.

The directional reflectance was obtained with a sample center-mounted in an 8-inch diameter integrating sphere reflectometer. The sphere coating was magnesium oxide. The sphere system is constructed so that the sample can be held in a horizontal position—a necessity for powders—while the sphere and external optics can be rotated so that angles of illumination or viewing up to approximately 75° can be obtained. The system can be evacuated to pressures in the 10⁻⁷ torr range.

The integrating sphere was operated in the reciprocal mode, that is, the sample was illuminated by diffuse light from the sphere walls. The directional reflectance $\rho(\theta)$ was obtained as the ratio of intensity when the sample was viewed to intensity when the wall was viewed (1). This measurement is equivalent (1) to illuminating the sample at an angle of incidence ψ equal to the angle of viewing θ . For the total or white light measurements a 1000 watt tungsten-iodine lamp (DXW) with a reflector was used. The detector was a Kipp-Zonen CA-1 thermopile. The spectral results were obtained with a Perkin-Elmer 112U spectrometer and a lead-sulfide cell detector.

Measurements were made on samples 10084,68 (powder), 10047,23 (basalt) (3), 10048,21 (breccia), and 10057,29 (crystalline). The spectral results are shown in Fig. 1 only for angles of 10° and 60°, but measurements for angles of viewing of 10°, 20°, 30°, 45°, and 60° were also obtained. All samples received were packaged in dry nitrogen.

The directional reflectance of the lunar powder shows no absorption bands over the spectral range studied. Sample 10084,68,1 was mounted in the integrating sphere and the system evacuated to pressures below 10⁻⁵ torr. Sample 10084,68,2 was run at atmospheric pressure 2 months after No. 1 sample and No. 2 had been resealed and stored in the original shipping container for these 2 months. The mea-

Table 1. Total directional reflectance of Apollo 11 material. The source was a 1000 watt DXW tungsten-iodine lamp.

Angle of viewing ψ	Sample				
	No. 10084,68,1		10057,29,1	10047,68,2	10048,21,1
	Vacuum run	Atmospheric run			
10°	0.102	0.098	0.137	0.118	0.162
20°	0.101	0.096	0.163	0.126	0.166
30°	0.117	0.103	0.145	0.124	0.168
45°	0.115	0.113	0.135	0.128	0.175
60°	0.148	0.135	0.129	0.129	0.183